

# Photoelectron Imaging and (2 + 1) Resonance Enhanced Multiphoton Ionization Spectroscopy Study of 2-Butanone Photoionization Dynamics<sup>†</sup>

Lei Shen, Bailin Zhang, and Arthur G. Suits\*

Department of Chemistry, Wayne State University, 5101 Cass Avenue, Detroit, Michigan 48202

Received: September 2, 2009; Revised Manuscript Received: December 10, 2009

(2 + 1) Resonance enhanced multiphoton ionization (REMPI) spectra were recorded for 2-butanone to study its photoionization dynamics. Two-photon excitation ( $53\ 200\text{--}55\ 000\text{ cm}^{-1}$  and  $57\ 000\text{--}59\ 500\text{ cm}^{-1}$ ) was used to prepare the molecule in the 3s and 3p Rydberg states, respectively. Vibrational transitions in the spectrum were assigned with the aid of ab initio calculations as well as photoelectron imaging results. Photoelectron imaging data in the 3s Rydberg region exhibits a vibrational progression in the CCOC deformation mode in the ionic state superimposed on an otherwise diagonal ( $\Delta\nu = 0$ ) ionization. Photoelectron imaging data in the 3p Rydberg region shows 3p–3s Rydberg–Rydberg mixing. The ionization energy obtained directly from the 3p photoelectron imaging is 9.541 eV.

## Introduction

There have been a number of spectroscopic investigations of simple aliphatic aldehydes recently, motivated both by the fact that they are model polyatomic systems where nonadiabatic dynamics are involved in photoionization and photodissociation and also because they are important intermediate species in isomerization reactions. We have recently reported ion and electron imaging studies of propanal<sup>1</sup> and iso-butanal<sup>2</sup> and acetaldehyde<sup>3</sup> by the DC sliced velocity map imaging technique.<sup>4,5</sup> 2-Butanone is an interesting related system and the subject of the present investigation. Phan et al.<sup>6</sup> reported the Raman and infrared spectra of 2-butanone in both gas phase and condensed media. Two stable conformers, *trans* and *gauche*, are reported for this molecule with the *trans* form more stable. Vacuum ultraviolet (VUV) absorption spectra<sup>7</sup> were recorded in the range between 135 and 200 nm, which covers the absorption of Rydberg states from the 3s to 7s region. The preliminary assignment in the VUV study provides a solid background for our UV (2 + 1) REMPI spectroscopy. The 2-butanone molecular geometry is shown in Figure 1. The geometry of its neutral ground state belongs to the C1 point group.

Photoelectron spectroscopy<sup>8,9</sup> has been used as an invaluable tool to investigate the electronic structure and ionization dynamics of molecules. The ionization process can generally be divided into two categories: direct and indirect ionization. In REMPI spectroscopy,<sup>10</sup> molecules are first excited to an intermediate Rydberg state, and then the absorption of an additional photon or photons induces ionization. In direct ionization, the excitation processes involve prompt removal of the promoted electron. In an indirect ionization, the molecule can be excited to a “superexcited state”,<sup>11</sup> a neutral state above the ionization limit. This is typically a Rydberg state converging to an electronically excited level of the ion. Autoionization may then proceed by coupling of this level to lower levels in the ionization continuum.<sup>12,13</sup>

Interaction between Rydberg states, or between Rydberg and valence states, is ubiquitous in polyatomic molecular systems. However, research into this field remains a daunting task.

Pump–probe approaches have been applied to investigate the properties of these intermediate states in decay of highly excited electronic states. The development of ultrafast laser probes makes it feasible to monitor the time evolution of these states directly by controlling the delay between the pump pulse and probe pulse while recording photoelectron spectra.<sup>14</sup> REMPI is a more convenient way and therefore more frequently applied approach to study these phenomena. Furthermore, REMPI combined with ion and electron imaging allows the simultaneous measurement of the kinetic energy and the angular distributions of the products, whether molecular fragments or photoelectrons. Therefore, time-resolved photoelectron imaging has become a powerful tool in both the gas phase and the condensed phase.<sup>15–17</sup>

The theoretical treatment of these phenomena may be considered even more challenging than the experimental problem, owing both to the multireference approach required and to the difficulty of treating Rydberg states and valence states on the same footing. Recent theoretical developments brought to bear on these issues include time-dependent density functional theory<sup>18</sup> and EOM (equation of motion)–CCSD<sup>19</sup> methods. In this article, we describe the application of these state-of-the-art techniques to investigate the interaction of Rydberg states in the photoionization dynamics of 2-butanone.

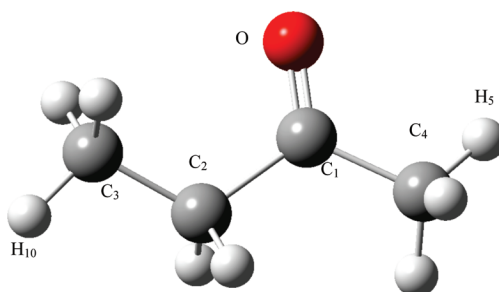
## Experimental and Computational Details

The velocity map imaging apparatus employed in this paper has been described in detail in previous publications.<sup>1,2</sup> Briefly, 2-butanone (Sigma Aldrich,  $\geq 99\%$ ) is used without further purification and expanded with helium at the backing pressure of  $\sim 3$  bar by a pulsed valve with a 1 mm orifice into the differentially pumped apparatus. After passing through a 1 mm diameter skimmer 30 mm downstream of the valve, the beam is collimated again by the hole on the repeller. It is perpendicularly crossed by the laser beam between the repeller and extractor ion optics.

Two sets of experiments are carried out to characterize the 3s and 3p Rydberg states of 2-butanone. In the (2 + 1) REMPI experiment, the laser wavelength was scanned from 363 to 376 nm and 336 to 351 nm (corresponding to  $53\ 200\text{--}55\ 000\text{ cm}^{-1}$

<sup>†</sup> Part of the “Benoit Soep Festschrift”.

\* Corresponding author. E-mail: asuits@chem.wayne.edu.

**Figure 1.** Geometry of neutral 2-butanone.

and 57 000–59 500 cm<sup>-1</sup> at the 2 photon level) to cover the 3s and 3p Rydberg series, respectively, based on the previous VUV study.<sup>7</sup> The UV light was generated by frequency doubling the output of a dye laser system (Scanmate, Lambda Physik) pumped by the second harmonic of a Nd:YAG laser (GCR 5). It was focused with a lens ( $f = 30$  cm) into the interaction region. The wavelength was calibrated by a wavemeter (Coherent Wavemaster). The mass-gated ion signal was recorded by a digital oscilloscope and captured on the computer.

In the electron imaging experiments, the electrons removed from the molecule due to the 2 + 1 REMPI process were recorded at selected wavelengths corresponding to peaks in the regions mentioned above. The laser polarization was set to be vertical in these experiments, parallel to the surface of the MCP detector. The electron kinetic energy distributions were obtained after the reconstruction from the 3D distribution by the basis set expansion (BASEX) inversion method.<sup>20</sup>

In addition to electron kinetic energy, imaging also readily provides the photoelectron angular distribution (PAD). The PAD provides valuable qualitative information about the ionization dynamics. In (2 + 1) REMPI, the angular distribution can be expressed as the function of the angle  $\theta$  between the laser polarization and outgoing electron  $\mathbf{k}$  vector

$$I(\theta) \cong 1 + \beta_2 P_2(\cos \theta) + \beta_4 P_4(\cos \theta) + \beta_6 P_6(\cos \theta) \quad (1)$$

where  $P_n(\cos \theta)$  represent the Legendre polynomial expansion in  $\cos \theta$ , and  $\beta_n$  are the anisotropy parameters.<sup>21</sup> The PAD from the 3s Rydberg ( $l = 0$ ) is expected to have a pure p type outgoing wave character due to the selection rule ( $\Delta l = \pm 1$ ), while the outgoing PAD for the 3p Rydberg should have the character of the mixture of s wave and d wave.

The equilibrium geometry and vibrational frequencies of neutral and ionic 2-butanone were calculated at B3LYP/6-311++G(2d, 2p) level. The excited states of the cation were calculated by TD-DFT/6-311++G(2d, 2p). The Gaussian 2003 package<sup>22</sup> was employed in these calculations. The excited states of the neutral 2-butanone were optimized by the EOM (equation of motion)-CCSD/6-311 (3+,+)G\* method using the Q-chem package.<sup>23</sup>

## Results

**Theoretical Calculations.** Figure 1 depicts the configuration of the more stable *trans* conformer of neutral 2-butanone. The geometric parameters of its neutral and ionic states are listed in Table 1. These values are consistent with previous microwave measurements.<sup>24</sup> There is a significant change from the neutral to the ionic state in the dihedral angle of OC<sub>1</sub>C<sub>2</sub>C<sub>3</sub>, which indicates that the OCCC deformation mode might be an active vibration in the ionization process.

**TABLE 1: Main Structural Parameters by Ab Initio Calculations<sup>a</sup>**

parameter	ground state	cation
$r(C=O)$	1.219	1.190
$r(C_1-C_2)$	1.524	1.578
$r(C_1-C_4)$	1.519	1.526
$r(C_2-C_3)$	1.527	1.510
$\angle(C_2C_1O)$	121.98	119.86
$\angle(C_2C_1C_4)$	116.69	117.94
$\angle(C_1C_2O_3)$	114.29	116.27
Dih <sup>b</sup> (CCCH <sub>3</sub> )	179.10	179.55
Dih(OC <sub>1</sub> C <sub>2</sub> C <sub>3</sub> )	-5.10	-15.8
Dih(C <sub>4</sub> CCO)	179.60	179.70
Dih(H <sub>10</sub> CCO)	179.10	179.55

<sup>a</sup> Bond length in Å and angles in degrees. The (U)B3LYP/6311++G(2d,2p) level was used in the calculations. <sup>b</sup> Dihedral angle.

**TABLE 2: Calculated Vibrational Frequencies (Unscaled, cm<sup>-1</sup>) of 2-Butanone and the 2-Butanone Cation<sup>a</sup>**

mode	approximate description	cation	ground
$\nu_1$	asymmetric torsion	59.7	21.2
$\nu_2$	CH <sub>3</sub> torsion (close to C=O)	109.7	101
$\nu_3$	CH <sub>3</sub> torsion	237.0	247.6
$\nu_4$	CO out-of-plane bend	468.1	588.7
$\nu_5$	CH <sub>2</sub> rock	742.7	759.2
$\nu_6$	CH <sub>3</sub> out-of-plane rock (C=O)	969.9	999.9
$\nu_7$	CH <sub>3</sub> out-of-plane rock	1067.9	1136.5
$\nu_8$	CH <sub>2</sub> twist	1253.4	1291.8
$\nu_9$	CH <sub>3</sub> antisymmetric deformation (C=O)	1458.1	1483.4
$\nu_{10}$	CH <sub>3</sub> antisymmetric deformation	1463.0	1498.7
$\nu_{11}$	CH <sub>2</sub> antisymmetric stretch	3082.4	3050.6
$\nu_{12}$	CH <sub>3</sub> antisymmetric stretch (C=O)	3125.7	3110.5
$\nu_{13}$	CH <sub>3</sub> antisymmetric stretch	3145.8	3117.7
$\nu_{14}$	C <sub>1</sub> C <sub>2</sub> C <sub>3</sub> bend	227.0	201.5
$\nu_{15}$	CC(O)C deformation	404.3	477.3
$\nu_{16}$	CO in-plane bend	341.0	402.6
$\nu_{17}$	C <sub>1</sub> C <sub>2</sub> C <sub>3</sub> symmetric stretch	568.8	758.9
$\nu_{18}$	C <sub>1</sub> C <sub>4</sub> stretch	806.6	940.9
$\nu_{19}$	C <sub>1</sub> C <sub>2</sub> C <sub>3</sub> antisymmetric stretch	943.1	958.8
$\nu_{20}$	CH <sub>3</sub> in-plane rock	1017.8	1108.0
$\nu_{21}$	CH <sub>3</sub> in-plane rock (C=O)	1082.0	1190.5
$\nu_{22}$	CH <sub>2</sub> wag	1281.6	1375.7
$\nu_{23}$	CH <sub>3</sub> symmetric deformation (C=O)	1341.2	1393.3
$\nu_{24}$	CH <sub>3</sub> symmetric deformation	1415.5	1423.5
$\nu_{25}$	CH <sub>2</sub> deformation	1431.2	1459.2
$\nu_{26}$	CH <sub>3</sub> antisymmetric deformation (C=O)	1435.9	1473.9
$\nu_{27}$	CH <sub>3</sub> antisymmetric deformation	1498.1	1506.9
$\nu_{28}$	C=O stretch	1683.3	1776.0
$\nu_{29}$	CH <sub>2</sub> symmetric stretch	3015.0	3016.5
$\nu_{30}$	CH <sub>3</sub> symmetric stretch (C=O)	3043.7	3038.6
$\nu_{31}$	CH <sub>3</sub> symmetric stretch	3040.0	3036.8
$\nu_{32}$	CH <sub>3</sub> antisymmetric stretch	3107.5	3089.3
$\nu_{33}$	CH <sub>3</sub> antisymmetric stretch (C=O)	3183.9	3144.9

<sup>a</sup> The (U)B3LYP/6311++G(2d,2p) level was used in the calculations.

Vibrational frequency calculations shown in Table 2 were performed on the neutral and the ion to aid in the assignment of the REMPI spectra. It would be more desirable to have the frequencies of the Rydberg states themselves since the vibrational transitions in the REMPI spectra correspond to the Rydberg state frequencies. However, this calculation is quite difficult; instead we rely on observed frequency trends in the change from neutral to ionic states, which for the most part should be closely related to those for the Rydbergs.

Although the vibrational frequency calculation is challenging, the energetics of the Rydberg states can be calculated by the EOM-CCSD method quite well. Table 3 lists the photon energy

**TABLE 3: Comparison of Experimental and Theoretical Results for One-Photon Excitation Wavelengths (nm) of  $n = 3$  Ry States and the Quantum Defect of 2-Butanone**

	3s	3p	3d
Exp(VUV) <sup>a</sup>	196.85(0.95)	170.32(0.54) 171.94(0.58)	160.51(0.26) 156.51(0.09)
theory	195.2(0.93)	173.6(0.61) 172.0(0.58) 170.5(0.55)	160.6(0.26) 157.7(0.15) 157.1(0.12) 156.2(0.08) 155.9(0.06)

<sup>a</sup> From ref 7.

required to access these excited states. These values agree very well with the numbers previously determined by the VUV spectra. The calculations were performed using the conventional 6-311++G basis set as well; however, the values obtained deviated considerably from the experiment. Therefore, the new basis set 6-311(3+,+)G\* was chosen. This clearly provides improved accuracy, as discussed in the recent study of diazomethane.<sup>25</sup>

**REMPI Spectra.** Figure 2 shows the 2 + 1 REMPI spectra of 2-butanone in the energy range 57 000–59 500 cm<sup>-1</sup> (a) and 53 200–55 000 cm<sup>-1</sup> (b) (energies at the two-photon level). The spectra were recorded in both parent ion and fragment  $m/z = 43$  conditions. The ion signal from the fragment was much stronger than the parent ion. In both figures, clear vibrational transitions can be resolved. The higher energy series peaks are quite broad, with linewidths implying lifetimes on the order of picoseconds or less. The assignment of these peaks will be discussed later.

**Photoelectron Imaging.** The results of the electron imaging experiment on selected transitions in the 3p and 3s region are shown in Figures 3 and 5, respectively. All the images in the 3p regime exhibit the same behavior: there are two intense rings which correspond to two dominant peaks in the electron kinetic energy distribution. There is a small peak at 1.388 eV in Figure 3C, which likely corresponds to the formation of the ground state cation. On the basis of this peak, the ionization energy of 2-butanone can be directly extracted as 9.541 eV. Photoelectron images in the 3s region show the progression of vibrational energy levels in the cation, and the intensity decreases gradually as the number of quanta increases. One image at 53 951.96 cm<sup>-1</sup>

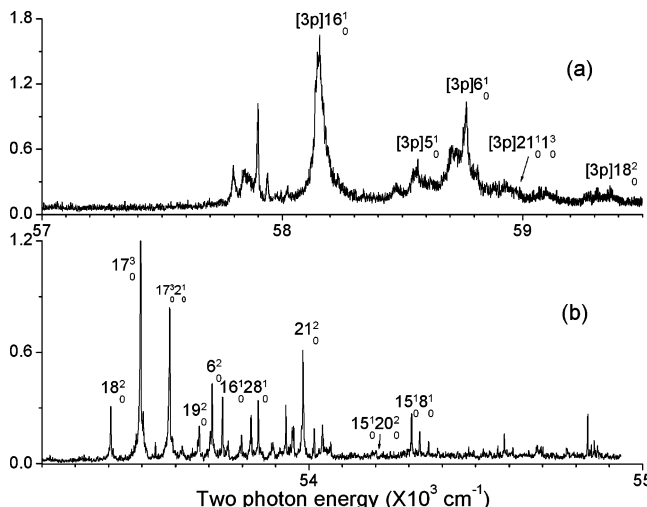


**Figure 2.** (2 + 1) Resonance enhanced multiphoton ionization (REMPI) spectra of 2-butanone through the (a) 3s and (b) 3p Rydberg states.

is particularly interesting because the inner part of the image is distinct from others. It has a strong slow electron release, and the angular distribution of the inner part ( $\beta_2 = 0.5$ ) is different from the outer rings ( $\beta_2 = 1.0$ ).

## Discussion

**Rydberg States of 2-Butanone.** From the EOM calculations, the two-photon excitation results in the promotion of electrons from the highest  $\pi$  orbital into the 3s and 3p Rydberg region. The excitation energies of the Rydberg series can be approximately represented by the Rydberg formula<sup>26</sup>

$$E_{\text{Ryd}} = \text{IE} - 109737.3/(n - \delta)^2 \text{ cm}^{-1} \quad (2)$$

Here,  $n$  is the principal quantum number;  $\delta$  is the quantum defect;  $E_{\text{Ryd}}$  is the excitation energy; and IE is the ionization energy. In an earlier study, the ionization potential of 2-butanone was determined to be 9.53 eV by photoelectron spectroscopy.<sup>27</sup> It is here measured more accurately by high-resolution photoelectron imaging to be 9.541 eV. The calculated quantum defect can be used to characterize the composition of the Rydberg states. Usually, it has the values of 0.9–1.2 for s-states, 0.3–0.9 for p-states, and smaller or equal to 0.1 for d-states.<sup>26</sup> The lowest ten excited states were obtained from the EOM–CCSD calculations; nine of these are Rydberg states and are listed in Table 3. For the first excited state with 270.5 nm excitation wavelength,  $\delta = 1.34$ . This value is too large for an s-state; it is likely not the lowest Rydberg state but instead an excited valence state. The excitation at 195.2 nm is thus assigned as the 3s Rydberg origin. Values of 173.6, 172.0, and 170.5 nm are the calculated excitation wavelengths of 3p (x, y, z) Rydberg states, respectively. The remaining five excitations belong to the 3d Rydberg series.

**Assignment of the REMPI Spectra.** The initial motivation of this study was to scan the REMPI spectrum in a wide range to search for transitions of two conformers of this molecule. Very clear vibronic transitions are observed in Figure 2(a) and (b). Since the origin of 3s ( $\sim 51$  229 cm<sup>-1</sup> from EOM–CCSD calculations) is out of the range of the scan, the vibrational spacing between these transitions and the 3s origin is unknown. A direct way to identify the transitions is to compare the vibrational spacing in the spectra with the ab initio frequency calculation of the Rydberg states. Since these calculations are not available, an indirect approach relying on ion frequencies and exploiting the photoelectron data must be applied. Previous photoelectron imaging studies on propanal<sup>1</sup> and isobutanal<sup>2</sup> showed that the strongest peak in the electron spectra generally represents the most probable vibrational mode of the cation as expected since the geometry of the Rydberg state resembles the ground state of the ion. The ab initio frequency calculation of the ground state cation is provided in Table 2. Thus, the photoelectron imaging data and the ab initio calculation can be used as a powerful combination to assign the spectra. The transition energies and assignments of vibronic bands are summarized in Table 4. The detailed assignment can be found in the analysis of the photoelectron imaging.

**Photoelectron Imaging through the 3p Rydberg.** Figure 3(A) is the photoelectron image recorded at 58 159.84 cm<sup>-1</sup>. The dominant fast peak is located about 285 cm<sup>-1</sup> away from the position where the production of the vibrationless ion is expected on the basis of the ionization energy determined above. According to the ab initio calculation, the frequency of  $\nu_{16}^+$  of the cation is 341 cm<sup>-1</sup> (unscaled). Therefore, this fast peak is

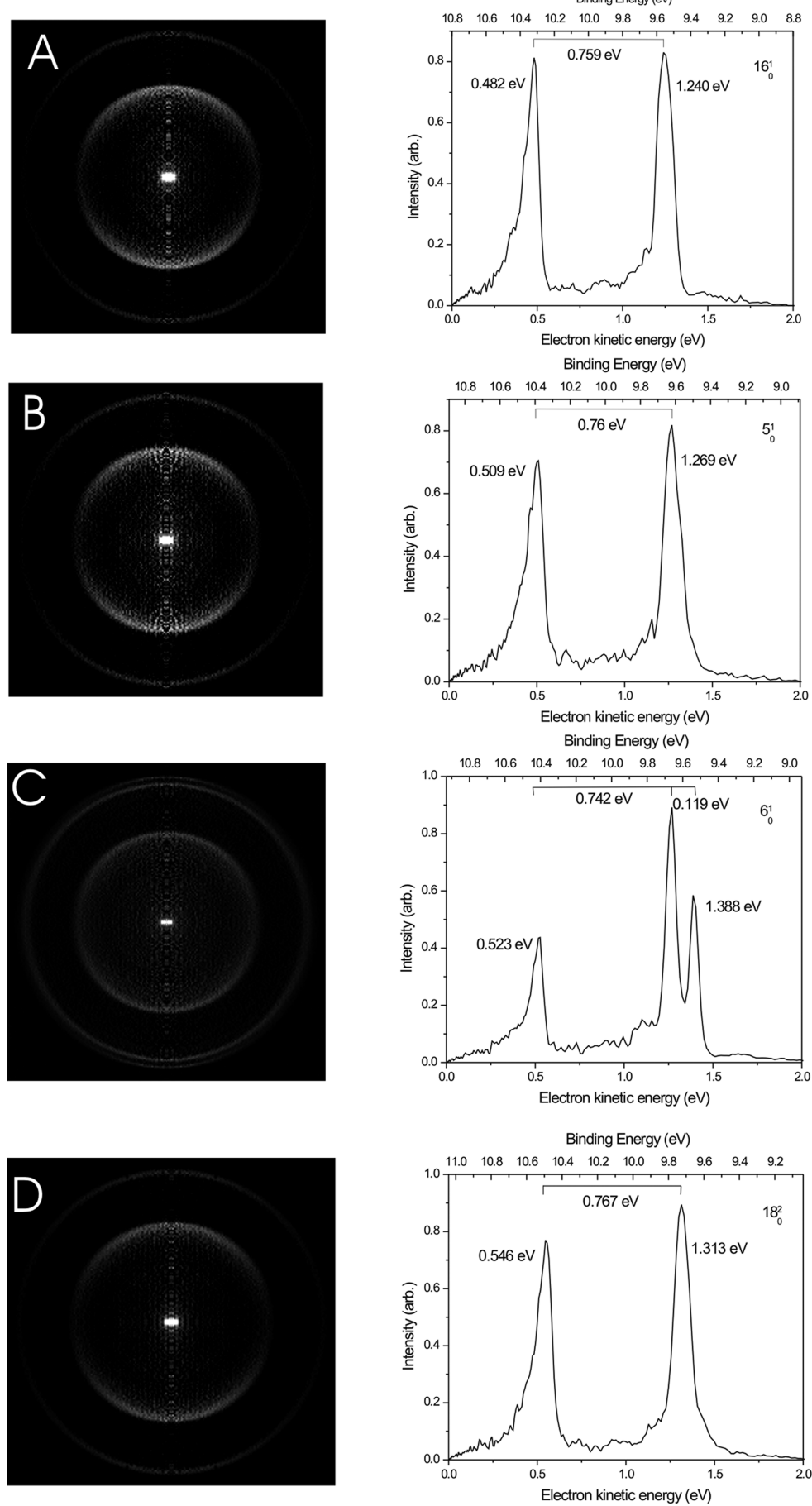


**Figure 3.** Photoelectron images and corresponding photoelectron spectra obtained after two-photon excitation via the 3p Rydberg state at (A)  $58\ 159.84\ \text{cm}^{-1}$ ; (B)  $58\ 559.60\ \text{cm}^{-1}$ ; (C)  $58\ 763.56\ \text{cm}^{-1}$ ; and (D)  $59\ 363.03\ \text{cm}^{-1}$ .

**TABLE 4: Transition Energies and Assignments of Vibronic Bands Observed in the (2 + 1) REMPI Spectra of 2-Butanone**

transition energy $2hv$ (cm $^{-1}$ )	assignments
53407.84	[3s]18 $^2_0$
53497.52	[3s]17 $^3_0$
53583.84	[3s]17 $^3_0$ 2 $^1_0$
53673.72	[3s]19 $^2_0$
53711.44	[3s]6 $^6_0$
53799.40	[3s]16 $^1_0$ 28 $^1_0$
53951.96	[3s]21 $^2_0$
54201.52	[3s]15 $^1_0$ 20 $^2_0$
54306.64	[3s]8 $^3_0$
58159.84	[3p]16 $^1_0$
58559.60	[3p]5 $^1_0$
58763.56	[3p]6 $^1_0$
58960.07	[3p]21 $^1_0$ 1 $^3_0$
59363.03	[3p]18 $^2_0$

assigned as one quantum of  $\nu_{16}^+$  excitation. Since the geometry of the Rydberg state resembles the ground ionic state, it is reasonable to assign this transition in the 3p REMPI spectrum as  $16_0^1$ . In the same way, the transition in Figure 3(B), 58 559.6 cm $^{-1}$ , is assigned as  $5_0^1$ ; the transition in Figure 3(C), 58 763.56 cm $^{-1}$ , corresponds to  $6_0^1$ , and in Figure 3(D), 59 363.03 cm $^{-1}$  is attributed to  $18_0^2$ .

The slow peak located 0.759 eV (6509 cm $^{-1}$ ) from the origin is mysterious, in that according to the Franck–Condon principle no vibrational excitation can account for this dominant peak. Hence, direct ionization from the 3p Rydberg state is not a plausible explanation for this feature. The first excited state of the cation is about 2.5 eV above the ground state based on a TD-DFT calculation. Therefore, the production of the electronically excited cation is not likely either. It is instead likely that interaction of the Rydberg states may account for this discrepancy. The nonadiabatic dynamics of such Rydberg states at near-degeneracy have been studied previously. The possible mechanism is illustrated in Figure 4. The 16 mode excited 3p Rydberg state can interconvert to a vibrationally excited 3s Rydberg state. This, followed by the absorption of the third photon, will result in Franck–Condon favored formation of a highly vibrationally excited cation. The electron energy difference will then roughly correspond to the difference in energy between the 3s and 3p Rydberg origins. This is based on the assumption that the vibrational spacing of the ion should resemble its Rydberg states. From the EOM–CCSD calculations, the energy difference between the 3s (51 229 cm $^{-1}$ ) and 3p (57 604 cm $^{-1}$ ) origins is 6385 cm $^{-1}$ , which is very close to the observed peak spacing.

The angular distributions of the two rings in the image are different, which indicates that the two peaks originate from different electronic states. This again supports the mechanism proposed above. Therefore, the slow peak in the 3p electron image is attributed to the 3s/3p Rydberg–Rydberg mixing. The other 3p images exhibit the same pattern with mainly two peaks: the fast peak can be attributed to the vibrationally excited 3p Rydberg state, while the slow peak originates from the 3s Rydberg state due to the 3p/3s Rydberg–Rydberg mixing.

**Photoelectron Imaging through the 3s Rydberg.** Selected photoelectron images from transitions in the 3s region are depicted in Figure 5. As shown in Figure 5(A), a dominant peak is located about 1540 cm $^{-1}$  away from the vibrationless cation (0.392 eV, calculated from the new IE). This energy gap matches well with 2 quanta excitation of  $\nu_{18}^+$  (806 cm $^{-1}$ , unscaled). Thus, the peak in the REMPI spectrum corresponding to this transition is assigned as  $18_0^2$ . There is a progression of two more peaks

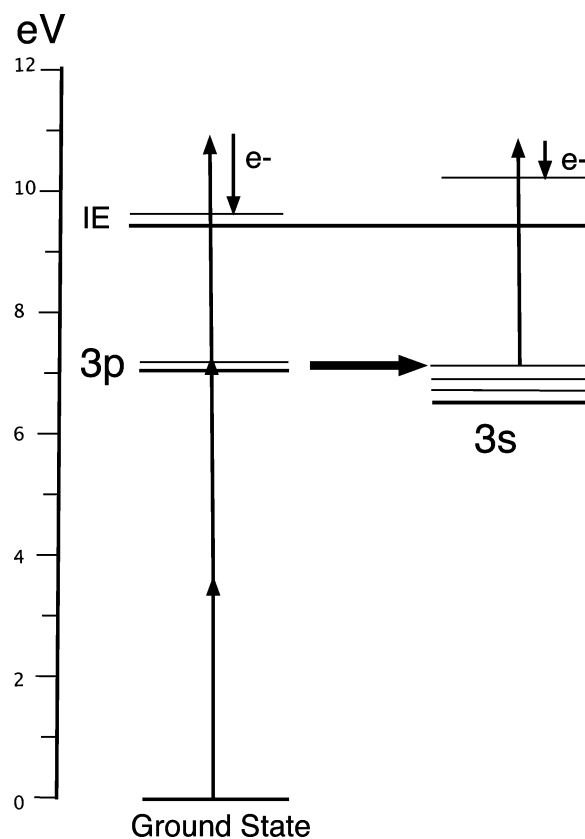


**Figure 4.** Schematic diagram illustrating the 3p/3s Rydberg–Rydberg mixing.

with 0.049 eV ( $\sim$ 403 cm $^{-1}$ ) spacing. From the ab initio calculation, the frequency of CCOC deformation ( $\nu_{15}^+$ ) of the cation is 404 cm $^{-1}$ . Hence this progression is believed to be the excitation of the backbone deformation mode of the cation. The observation of the non-Franck–Condon vibrational progressions has been discussed above. The active backbone deformation mode induces a geometrical change of molecule, which results in the nondiagonal transitions between the 3s Rydberg state and ground ionic state. The ab initio result also confirms this conclusion since the value of the frequency of this mode changes significantly upon ionization. All the other images show this identical progression. In the same way, the transition in Figure 5(B) can be assigned as  $6_0^1$ , and the transition in Figure 5(D) is  $15_0^1$ 20 $_0^2$ .

The electron image at 53 951.96 cm $^{-1}$  has a striking slow component. There are two sharp peaks at 0.005 and 0.034 eV in addition to the  $\nu_{15}^+$  progression. The angular distribution of the slow component is different from the fast part, which indicates that they must originate from different ionization pathways. There are several possibilities that may account for the production of the internally hot cation. First of all, if the cation is produced in both the ground state and the electronically excited state the electron corresponding to the excited state cation will have low kinetic energy release. However, the result from our TD-DFT calculation shows that the lowest lying electronic state is about 2.5 eV above the ground state, which is much larger than the spacing between the peaks ( $\sim$ 0.2 eV). Therefore, this possibility is excluded. Another possibility is the coupling of the 3s Rydberg to the lowest excited valence state of neutral butanone, which may also result in the slow electron. The energetics from the EOM–CCSD calculation show that the excitation to the valence state is 270.5 nm, but that to the 3s Rydberg is 195.2 nm. This 1.78 eV energy difference is too large compared to the peak spacing as well.

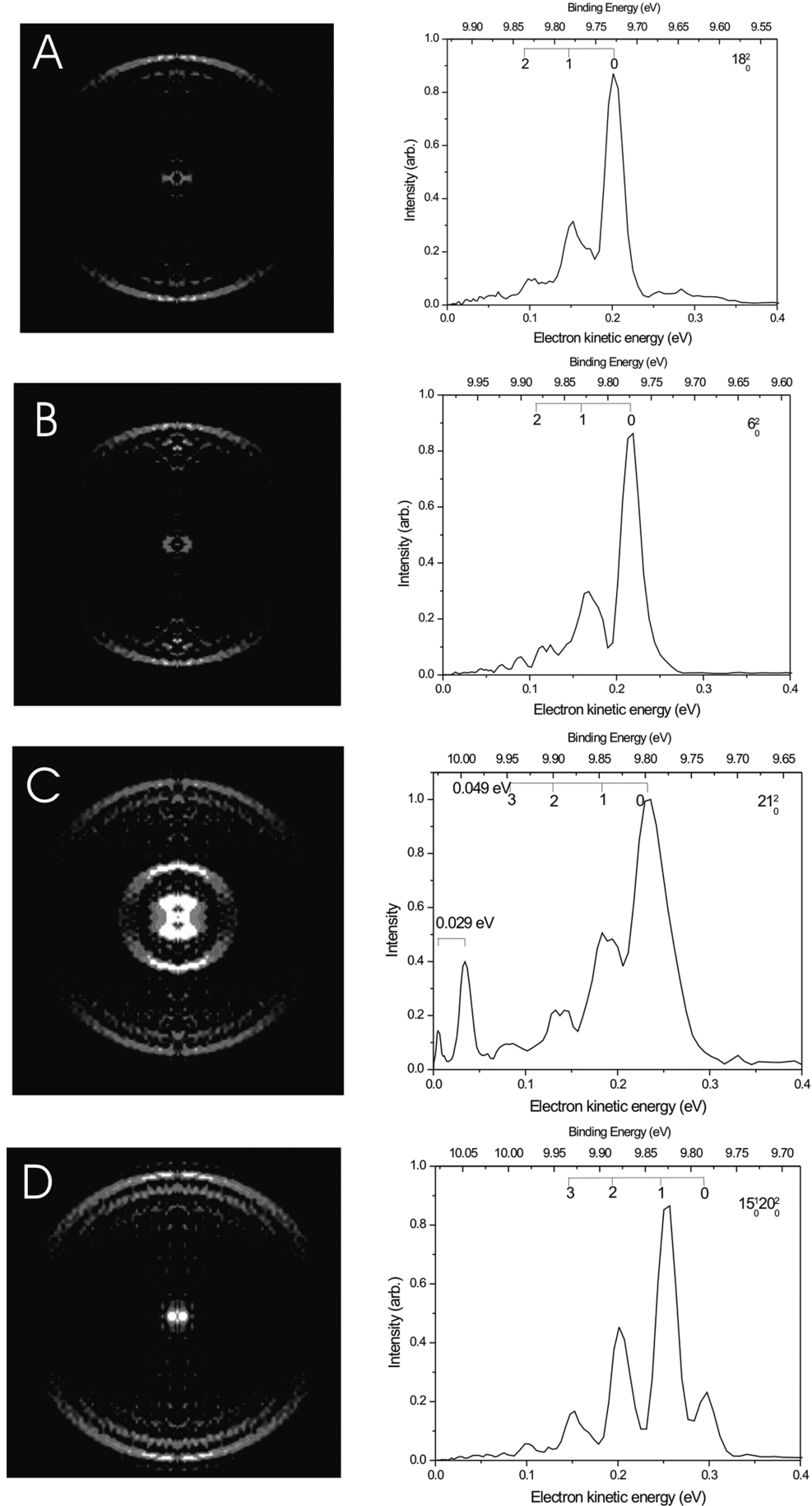


**Figure 5.** Photoelectron images and corresponding photoelectron spectra after two-photon excitation via the 3s Rydberg state at (A)  $53\ 407.84\text{ cm}^{-1}$ ; (B)  $53\ 711.44\text{ cm}^{-1}$ ; (C)  $53\ 951.96\text{ cm}^{-1}$ , and (D)  $54\ 201.52\text{ cm}^{-1}$ .

Strong slow peak distributions have been observed in the photoelectron study of a number of systems: NO,<sup>28</sup> N<sub>2</sub>O,<sup>29</sup> CO,<sup>30</sup> HCl,<sup>31</sup> and HBr.<sup>32</sup> Since the direct ionization mechanism cannot explain this slow feature, indirect ionization mechanisms are proposed instead. If the photon energy is sufficient, molecules may be first excited to an intermediate “superexcited state” above the ionization limit. This superexcited state can autoionize if it is coupled to the ground state of the cation, resulting in internally excited ions.

Pure vibrational autoionization cannot account for the two sharp peaks due to the propensity rule  $\delta\nu = -1$  in vibrational autoionization. Moreover, the  $\beta$  parameter of the outer rings is consistent, while that for the slow component is completely different. This difference in the angular distribution again implies that there might be other electronic states involved in this ionization process. Therefore, electronic autoionization (near resonance autoionization<sup>33</sup>) of the superexcited states likely accounts for the particular intense appearance of low kinetic energy release peaks. It is difficult to identify the superexcited states that are involved in this interaction. More theoretical work on the details of the excited states of this molecule is required to elucidate the underlying mechanism.

## Conclusions

2-Butanone photoionization dynamics have been studied by the combination of (2 + 1) REMPI spectroscopy and photoelectron imaging. The REMPI/imaging technique allows us to access the intermediate 3s and 3p Rydberg and valence states. The photoelectrons resulting from REMPI are collected by the velocity map imaging technique that provides the simultaneous measurement of the energy release and the angular distribution.

Clear vibrational structures are observed in the REMPI spectra, and assignments are made based on the photoelectron images as well as ab initio frequency calculations. Biomodal kinetic energy distributions are seen in the 3p electron images: the fast peak is due to the Franck–Condon favorable diagonal transition, while the slow peak results from the 3s/3p Rydberg–Rydberg mixing. Electron images in the 3s region consistently show a progression of the CCOC deformation mode. Electronic autoionization of the superexcited states is proposed to account for the near zero kinetic energy release in the image of 53 951.96 cm<sup>-1</sup>. Further theoretical work is required to elucidate the detailed mechanism.

**Acknowledgment.** This work was supported by the National Science Foundation under award number CHE-0715300. Additional calculations were performed using the resources of the iOpenShell Center for Computational Studies of Electronic Structure and Spectroscopy of Open-Shell and Electronically Excited Species (<http://iopenshell.usc.edu>) supported by the National Science Foundation through the CRIF:CRF program. The authors thank Prof. Anna I. Krylov for providing that resource.

## References and Notes

- (1) Kim, M. H.; Shen, L.; Suits, A. G. *Phys. Chem. Chem. Phys.* **2006**, 8, 2933.
- (2) Shen, L.; Singh, P. C.; Kim, M.; Zhang, B. L.; Suits, A. G. *J. Phys. Chem. A* **2009**, 113, 68.
- (3) Lee, S. K.; Silva, R.; Kim, M. H.; Shen, L.; Suits, A. G. *J. Phys. Chem. A* **2007**, 111, 6741.
- (4) Chandler, D. W.; Houston, P. L. *J. Chem. Phys.* **1987**, 87, 1445.
- (5) Eppink, A.; Parker, D. H. *Rev. Sci. Instrum.* **1997**, 68, 3477.
- (6) Durig, J. R.; Feng, F. S.; Wang, A. Y.; Phan, H. V. *Can. J. Chem.* **1991**, 69, 1827.
- (7) Otoole, L.; Brint, P.; Kosmidis, C.; Boulakis, G.; Tsekeris, P. *J. Chem. Soc., Faraday Trans.* **1991**, 87, 3343.
- (8) Eland, J. H. D. *Photoelectron spectroscopy; an introduction to ultraviolet photoelectron spectroscopy in the gas phase*; Butterworths: London, 1974.
- (9) Rabalais, J. W. *Principles of ultraviolet photoelectron spectroscopy*; Wiley: New York, 1977.
- (10) Anderson, S. L. *Adv. Chem. Phys.* **1992**, 82, 177.
- (11) Platzman, R. L. *J. Phys. Radium* **1960**, 21, 853.
- (12) Golovin, A. V.; Heiser, F.; Quayle, C. J. K.; Morin, P.; Simon, M.; Gessner, O.; Guyon, P. M.; Becker, U. *Phys. Rev. Lett.* **1997**, 79, 4554.
- (13) Nakamura, H. *Int. Rev. Phys. Chem.* **1991**, 10, 123.
- (14) Zewail, A. H. *J. Phys. Chem. A* **2000**, 104, 5660.
- (15) Suzuki, T.; Wang, L.; Kohguchi, H. *J. Chem. Phys.* **1999**, 111, 4859.
- (16) Neumark, D. M. *Annu. Rev. Phys. Chem.* **2001**, 52, 255.
- (17) Stolow, A. *Annu. Rev. Phys. Chem.* **2003**, 54, 89.
- (18) Marques, M. A. L.; Gross, E. K. U. *Annu. Rev. Phys. Chem.* **2004**, 55, 427.
- (19) Krylov, A. I. *Annu. Rev. Phys. Chem.* **2008**, 59, 433.
- (20) Dribinski, V.; Ossaditchi, A.; Mandelshtam, V. A.; Reisler, H. *Rev. Sci. Instrum.* **2002**, 73, 2634.
- (21) Suzuki, T.; Whitaker, B. J. *Int. Rev. Phys. Chem.* **2001**, 20, 313.
- (22) Frisch, M. J.; Trucks, G. W.; Schlegel, H. B.; Scuseria, G. E.; Robb, M. A.; Cheeseman, J. R.; Montgomery, J. A., Jr.; Vreven, T.; Kudin, K. N.; Burant, J. C.; Millam, J. M.; Iyengar, S. S.; Tomasi, J.; Barone, V.; Mennucci, B.; Cossi, M.; Scalmani, G.; Rega, N.; Petersson, G. A.; Nakatsuji, H.; Hada, M.; Ehara, M.; Toyota, K.; Fukuda, R.; Hasegawa, J.; Ishida, M.; Nakajima, T.; Honda, Y.; Kitao, O.; Nakai, H.; Klene, M.; Li, X.; Knox, J. E.; Hratchian, H. P.; Cross, J. B.; Bakken, V.; Adamo, C.; Jaramillo, J.; Gomperts, R.; Stratmann, R. E.; Yazyev, O.; Austin, A. J.; Cammi, R.; Pomelli, C.; Ochterski, J. W.; Ayala, P. Y.; Morokuma, K.; Voth, G. A.; Salvador, P.; Dannenberg, J. J.; Zakrzewski, V. G.; Dapprich, S.; Daniels, A. D.; Strain, M. C.; Farkas, O.; Malick, D. K.; Rabuck, A. D.; Raghavachari, K.; Foresman, J. B.; Ortiz, J. V.; Cui, Q.; Baboul, A. G.; Clifford, S.; Cioslowski, J.; Stefanov, B. B.; Liu, G.; Liashenko, A.; Piskorz, P.; Komaromi, I.; Martin, R. L.; Fox, D. J.; Keith, T.; Al-Laham, M. A.; Peng, C. Y.; Nanayakkara, A.; Challacombe, M.; Gill, P. M. W.; Johnson, B.; Chen, W.; Wong, M. W.; Gonzalez, C.; Pople, J. A. *Gaussian 03*, revision C.02; Gaussian, Inc.: Wallingford, CT, 2004.
- (23) Kong, J.; White, C. A.; Krylov, A. I.; Sherrill, D.; Adamson, R. D.; Furlani, T. R.; Lee, M. S.; Lee, A. M.; Gwaltney, S. R.; Adams, T. R.; Ochsenfeld, C.; Gilbert, A. T. B.; Kedziora, G. S.; Rassolov, V. A.; Maurice, D. R.; Nair, N.; Shao, Y. H.; Besley, N. A.; Maslen, P. E.; Dombroski, J. P.; Daschel, H.; Zhang, W. M.; Korambath, P. P.; Baker, J.; Byrd, E. F. C.; Van Voorhis, T.; Oumi, M.; Hirata, S.; Hsu, C. P.; Ishikawa, N.; Florian, J.; Warshel, A.; Johnson, B. G.; Gill, P. M. W.; Head-Gordon, M.; Pople, J. A. *J. Comput. Chem.* **2000**, 21, 1532.
- (24) Pierce, L.; Chang, C. K.; Hayashi, M.; Nelson, R. *J. Mol. Spectrosc.* **1969**, 32, 449.
- (25) Fedorov, I.; Koziol, L.; Li, G. S.; Parr, J. A.; Krylov, A. I.; Reisler, H. *J. Phys. Chem. A* **2007**, 111, 4557.
- (26) Sandorfy, C. *The role of Rydberg states in spectroscopy and photochemistry: low and high Rydberg states*; Kluwer Academic: Dordrecht; Boston, 1999.
- (27) Traeger, J. C. *Org. Mass Spectrom.* **1985**, 20, 223.
- (28) Kimman, J.; Kruit, P.; Vanderwiel, M. *J. Chem. Phys. Lett.* **1982**, 88, 576.
- (29) Guyon, P. M.; Baer, T.; Nenner, I. *J. Chem. Phys.* **1983**, 78, 3665.
- (30) Katayanagi, H.; Matsumoto, Y.; de Lange, C. A.; Tsubouchi, M.; Suzuki, T. *J. Chem. Phys.* **2003**, 119, 3737.
- (31) Romanescu, C.; Manzhos, S.; Boldovsky, D.; Clarke, J.; Loock, H. P. *J. Chem. Phys.* **2004**, 120, 767.
- (32) Romanescu, C.; Loock, H. P. *Phys. Chem. Chem. Phys.* **2006**, 8, 2940.
- (33) Powis, I.; Baer, T.; Ng, C. Y. *High resolution laser photoionization and photoelectron studies*; Wiley: Chichester [England]; New York, 1995.